The rotational spectrum and hyperfine structure of the methylene radical CH_2 studied by far-infrared laser magnetic resonance spectroscopy[a)]

Trevor J. Sears, P. R. Bunker, and A. R. W. McKellar

Herzberg Institute of Astrophysics, National Research Council of Canada, Ottawa, Ontario, Canada K1A 0R6

K. M. Evenson and D. A. Jennings

National Bureau of Standards, Boulder, Colorado 80303

J. M. Brown

Department of Chemistry, University of Southampton, Southampton SO9 5NH, United Kingdom
(Received 17 June 1982; accepted 25 August 1982)

Thirteen pure rotational transitions of CH_2 in its $\tilde{X}\,^3B_1$ ground vibronic state have been measured and assigned using the technique of far-infrared laser magnetic resonance (LMR) spectroscopy. The energy levels thus determined led to the prediction and subsequent detection by microwave spectroscopy of a further rotational transition 4_{04}–3_{13}, at lower frequency (~70 GHz). The analysis of these observations yields precise rotational constants as well as spin–spin, spin-rotation, and hyperfine interaction parameters for gas phase CH_2. Its rotational spectrum may enable interstellar CH_2 to be detected by radio astronomy. Two rotaional transitions within the $v_1 = 1$ excited vibrational state have also been identified in the LMR spectrum. Future observations of vibrationally excited CH_2 may afford a means of determining the singlet–triplet splitting in methylene, and studies of CD_2 and CHD will result in improved structural determinations.

I. INTRODUCTION

The methylene radical CH_2 is of great interest because of its importance both in spectroscopy and in chemistry. Spectroscopically, it is the simplest neutral polyatomic molecule with a triplet electronic ground state, and chemically it is the prototypical carbene. In the present paper, we report the measurement and analysis of the pure rotational laser magnetic resonance (LMR) spectrum of gas phase CH_2 which establishes for the first time the detailed geometrical and electronic structure of methylene in its ground electronic state.

The spectroscopic characterization of methylene has been a slow and difficult process; the first spectroscopic identification of CH_2 was reported by Herzberg and Shoosmith[1] in 1959. Herzberg[2] later analyzed the vacuum ultraviolet absorption spectrum and concluded that the ground electronic state was a triplet and that the structure was linear, or nearly so. The absorption spectrum from the lowest singlet state was studied in more detail by Herzberg and Johns,[3] who established that the $\tilde{a}\,^1A_1$ state is strongly bent whereas the $\tilde{b}\,^1B_1$ state is more nearly linear, with a bond angle of around 140°. More experimental information on CH_2 was forthcoming in the early 1970's with the observation of its ESR spectrum, obtained in rare gas matrices at low temperatures. Bernheim *et al.*[4] first observed the ESR spectrum, and concluded from the small apparent value of the anisotropic part of the spin–spin interaction that CH_2 in the $\tilde{X}$ state is very nearly linear. Soon afterwards, Wasserman *et al.*[5–8] published a series of papers showing that the apparent small anisotropic spin splitting parameter was a consequence of nearly free rotation about the molecular a axis in the matrix. Their interpretation implied a bent structure with an angle of about 136°. Subsequently, Herzberg and Johns[9] suggested that the ultraviolet absorption spectra of CH_2, CHD, and CD_2 could be rationalized in terms of a bent structure if one assumed that spectral lines involving $K_a > 0$ in the upper electronic state were broadened by predissociation and therefore not observed.

This interpretation of the ESR and ultraviolet spectra brought experiment into agreement with the large body of theoretical work existing at that time which strongly supported the bent structure for the ground state of CH_2.[10] A review of the theoretical work prior to about 1970 is given by Harrison and Allen[11] and later reviews have been written by Harrison[12] and Langhoff and Kern.[13] Recent *ab initio* calculations[10,14] agree that the lowest electronic state is indeed $^3B_1$ with a shallow energy minimum at an equilibrium HCH angle of $134 \pm 2°$.

The triplet fine structure of the ground state of methylene is expected to be dominated by the spin–spin dipolar terms which involve two zero-field splitting parameters D and E (see Sec. III below). The article by Langhoff and Kern[13] is primarily concerned with the *ab initio* calculation of these fine structure parameters. The two parameters can in principle be measured directly in the ESR experiments, and it is the magnitude of the anisotropic spin-splitting parameter E which establishes that the molecule is bent (this parameter is zero in a linear molecule). Prior to the present work, there was reasonable agreement between the best experimental[8] ESR ($D = 0.76 \pm 0.62$ cm^{-1}, $E = 0.052 \pm 0.017$ cm^{-1}) and theoretical[14] *ab initio* ($D = 0.807$ cm^{-1}, $E = 0.050$ cm^{-1}) estimates for these parameters, and one could be quite sure that the precise parameters for

[a)]Work supported in part by NASA contract W-15, 047.

 021-9606/82/235348-15$02.10

the isolated molecule would be fairly close to these values. This is indeed the case, as we show in Sec. IV of this paper. For a freely rotating molecule in the gas phase, there are additional contributions to the fine structure splittings arising from the spin-rotation interaction. This interaction is actually expected to be dominated by second order spin-orbit mixing of excited triplet states and is therefore likely to be small, since the first excited triplet state is at a rather high energy ($\approx 70\,000$ cm^{-1}) in CH_2. Spin-rotation coupling is considered in more detail in Sec. III.

Although there is reasonable agreement between theory and experiment on the geometrical and electronic structure of the ground state of CH_2, there is still controversy regarding the relative energies of the triplet and singlet electronic states. Most recent *ab initio* calculations[15,16] suggest that the first excited singlet state $\tilde{a}\,^1A_1$ lies about 0.45–0.50 eV (10–11 kcal mol^{-1}, or 3600–4100 cm^{-1}) above the $^3B_1$ ground state. This quantity has been obtained indirectly using photochemical and thermochemical arguments,[17–19] and these results agree approximately with the theoretical values. The first direct measurement of the singlet-triplet splitting in methylene came[20] from the photoelectron spectrum of CH_2^-,[1] and it was disconcerting to find that the derived value 0.845 eV was rather different from the expected one. Alternative interpretations[15] of the photoelectron spectrum invoked the possibility that photodetachment might arise from vibrationally hot CH_2^-, and these lead to estimates of the singlet-triplet splitting which are closer to the theoretical values. However, a careful re-examination[21] of the photoelectron data by the original workers did not support the hot band hypothesis, and left the discrepancy in the singlet-triplet splitting unexplained. Further study of the singlet–singlet absorption spectrum of CH_2[22] by laser induced fluorescence has not significantly altered the experimental situation.

In 1979, Mucha *et al.*[23] reported the detection of pure rotational transitions within the ground state of CH_2 by laser magnetic resonance. The identification of the spectrum as due to CH_2 rested on chemical evidence and on the observed triplet hyperfine structure, but at the time it was not possible to assign the rotational transition responsible for the spectrum, and thus no structural information could be obtained. A breakthrough in the spectroscopy of triplet CH_2 occurred very recently with the observation and assignment by Sears *et al.*[24] of transitions in the ν_2 (bending) fundamental band using CO_2 LMR in the 11 μm region. The search for this spectrum and its assignment were suggested and guided by the results of calculations which used the *ab initio* potential curve of Harding and Goddard[15(a)] together with the semirigid bender Hamiltonian of Bunker and Landsberg.[25] Earlier estimates of the bending frequency for CH_2, based on a harmonic approximation, were in the 1100 to 1200 cm^{-1} range, but the semirigid bender calculation gave a value of 992 cm^{-1}. This result encouraged the search for the ν_2 band by CO_2 LMR spectroscopy. The analysis of these LMR results gives an experimental value of $\nu_2 = 963$ cm^{-1}; the ν_2 band spectrum will be described in detail in a separate publication.[26]

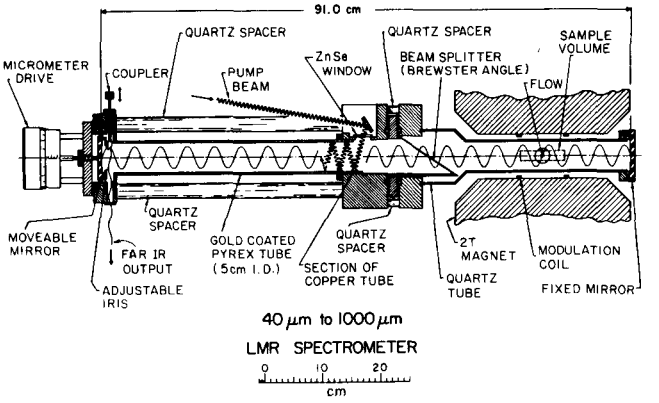

FIG. 1. Schematic diagram of the intracavity far-infrared laser magnetic resonance apparatus at the Natl. Bur. Stand., Boulder, Colorado.

Our preliminary analysis[24] of the 11 μm LMR spectrum gave spin-splitting parameters and also made it possible to refine the potential function used in the semirigid bender calculation, so that the frequencies of pure rotational transitions of CH_2 in the far-infrared could be predicted with reasonable accuracy. The present paper reports the observation and assignment of most of the allowed rotational transitions between the low lying levels ($E < 500$ cm^{-1}) of the radical. The spectra were recorded using the technique of far-infrared LMR. On the basis of these LMR results, it was possible to predict the frequencies for 4_{04}–3_{13}, the only rotational transition in the ground state which is accessible using conventional microwave techniques. The strongest components of this transition, which occur around 70 GHz, were subsequently detected by Lovas *et al.*[27] These microwave measurements are combined here with the LMR data in an appropriately weighted least-squares fit to determine rotational, centrifugal distortion, fine structure, and hyperfine parameters for CH_2 in its ground vibronic state. Interestingly, the analysis indicates that the published LMR spectrum of Mucha *et al.*[23] is not due to the ground vibrational state, but rather due to a transition within the $(v_1v_2v_3) = (100)$ excited vibrational state of CH_2. The rotational spectrum will allow a search to be made for CH_2 in astrophysical sources by millimeter astronomy. Our analysis also opens up the possibility of monitoring the kinetics of chemical reactions involving triplet CH_2 by using the LMR to monitor the radical concentration.

II. EXPERIMENTAL DETAILS

The spectra were recorded at the Boulder laboratories of the NBS using a new FIR (far-infrared) LMR spectrometer which is about five times more sensitive, allows more lines to lase, and is significantly easier to operate than its predecessor.[28] The spectrometer is shown in Fig. 1. A new 38 cm electromagnet with ring-shaped Hyperco pole caps produces a 7.5 cm homogeneous field region which is five times longer along the laser axis than previously,[28] accounting for the sensitivity increase. The new FIR laser cavity is 25 cm shorter and should oscillate to wavelengths well over 1000 μm. Better overlap between the pump and FIR

lasers yields a larger number of FIR lines. The improved overlap is accomplished with a nearly confocal mirror geometry, the insertion of the CO_2 pump at the beam waist, and the use of a cylindrical gold-plated Pyrex tube as the CO_2 laser reflector. This tube was found to double the output power in a FIR laser when compared to flat-sided mirrors. A section of 10 cm i.d. gold-coated copper tube is used as the first CO_2 beam focuser to begin a series of consecutive refocuses of the pump beam. Quartz is used for the cavity spacers in the spectrometer to provide good thermal stability. The beam splitter (see Fig. 1) is rotatable about the laser axis so the polarization can be rotated. The magnet is controlled by a rotating coil and is calibrated periodically with an NMR gaussmeter; the overall fractional uncertainty is $\pm 1\times10^{-4}$ above 0.1 T and 10^{-5} below 0.1 T [1 T(Tesla) = 10^4 G(Gauss)].

Methylene was produced in the spectrometer sample volume by the reaction of fluorine atoms with methane in a flow system, and the F atoms were obtained by passing a mixture of He and F_2 through a microwave discharge. The partial pressures were about 50, 1, and 0.5 Pa (1 Pa = 7.5 mTorr), respectively, for He, F_2, and CH_4. Essentially the same reaction has also been used to produce FIR LMR spectra of the species C, CH, C_2H, CF, and CH_2F.[28]

III. THEORY

The energies of the rotational levels for the ground vibronic state of CH_2 are the eigenvalues of the appropriate effective Hamiltonian. The form of this Hamiltonian for an asymmetric rotor molecule in a nonsinglet electronic state has been given by a number of authors,[29–31] and for triplet CH_2 it is

$$H_{\rm eff} = H_r + H_{\rm cd} + H_{\rm ss} + H_{\rm sr} + H_{\rm hfs} + H_z \ . \tag{1}$$

The first term H_r is the rigid rotor Hamiltonian given (in $\rm cm^{-1}$) by

$$H_r = AN_a^2 + BN_b^2 + CN_c^2 \ , \tag{2}$$

where A, B, and C are the rotational constants and N is the rotational angular momentum operator in units of $\hbar$. The second term $H_{\rm cd}$ accounts for centrifugal distortion, and adopting the "A" reduced form[32] of the operator, it is

$$\begin{aligned} H_{\rm cd} = &-\Delta_N \mathbf{N}^4 - \Delta_{NK}\mathbf{N}^2N_a^2 - \Delta_K N_a^4 - 2\delta_N\mathbf{N}^2(N_b^2 - N_c^2) - \delta_K[N_a^2, (N_b^2 - N_c^2)]_+ \\ &+ \Phi_N\mathbf{N}^6 + \Phi_{NK}\mathbf{N}^4N_a^2 + \Phi_{KN}\mathbf{N}^2N_a^4 + \Phi_K N_a^6 + 2\phi_N\mathbf{N}^4(N_b^2 - N_c^2) + \phi_{NK}\mathbf{N}^2[N_a^2, (N_b^2 - N_c^2)]_+ + \phi_K[N_a^4, (N_b^2 - N_c^2)]_+ \ . \end{aligned} \tag{3}$$

The next two terms $H_{\rm ss}$ and $H_{\rm sr}$ represent the fine structure interactions. First, the spin–spin dipolar Hamiltonian, expressing the interaction between the two unpaired electrons, which is[30]

$$H_{\rm ss} = (D/3)[2S_a^2 - S_b^2 - S_c^2] + E[S_b^2 - S_c^2] \ . \tag{4}$$

(The parameters D and E are related to the parameters α and β of Raynes[30] by $D = 3\alpha$ and $E = \beta$.) Second, the spin-rotation interaction, which is[33]

$$H_{\rm sr} = \epsilon_{aa}N_aS_a + \epsilon_{bb}N_bS_b + \epsilon_{cc}N_cS_c \ . \tag{5}$$

Centrifugal distortion corrections[33] to $H_{\rm sr}$ were found to be negligible in this work. The last term in the zero-field Hamiltonian is $H_{\rm hfs}$, representing the hyperfine interaction between the unpaired electron spins and the net nuclear spins of the two equivalent protons. This interaction represents the smallest contribution to the energy and its effects were neglected until the final stage of the analysis; it can be written[31]

$$H_{\rm hfs} = a_{FC}\mathbf{S}\cdot\mathbf{I} + \mathbf{S}\cdot\mathbf{T}\cdot\mathbf{I} \ . \tag{6}$$

Here the first term represents the isotropic Fermi contact interaction and the second term represents the dipolar interaction between the protons and the unpaired electron spins. The traceless dipolar hyperfine tensor T has two determinable diagonal elements, for example $T_{aa} = -(T_{bb} + T_{cc})$ and $T_{bb} = -(T_{aa} + T_{cc})$ and one off-diagonal element T_{ab}. The latter causes a mixing of *ortho* and *para* nuclear spin states but is not generally determinable because it requires an accidental near degeneracy of states with K_a differing by 1 to manifest itself. The detailed form of the operator is discussed by Bowater *et al.*[31]

Finally, we must take into account the energy of the interaction of the molecule with an external magnetic field; this is represented by the term[31]

$$H_z = \mu_B\mathbf{B}\cdot\mathbf{g}_s\cdot\mathbf{S} + \mu_B\mathbf{B}\cdot\mathbf{g}_r\cdot\mathbf{N} \ , \tag{7}$$

where $\mathbf{B}$ is the applied field, and μ_B is the Bohr magneton. The first term represents the isotropic and anistropic interactions of the electron spin with the field, and the second term represents the rotational Zeeman effect. The very small nuclear Zeeman term was not included after numerical tests showed its effects to be negligible.

The matrix of the Hamiltonian $H_{\rm eff}$ was set up in a fully-coupled prolate symmetric top basis set $|NKSJIFM_F\rangle$ and diagonalized numerically. The zero-field problem was treated exactly, but the matrix of the full Hamiltonian including the Zeeman terms is, in principle, infinite.

Various approximations were used in different stages of the analysis. After assignment of the first rotational transition (2_{11}–2_{02}), further assignments were made on the basis of the semirigid bender fit to this transition and to the ν_2 band data.[24,26] These predictions, which neglected spin splitting, were always within 2 $\rm cm^{-1}$ of the actual positions of the observed rotational transitions. Next, the Zeeman patterns for each transition were predicted using spin splittings from preliminary ν_2 band LMR fits and calculating the Zeeman shifts by considering only the isotropic electron spin part of the Zeeman operator (7). This calculation required the diagonalization of matrices given by the expressions[35]:

$$\langle F_1|H|F_1\rangle = E_1 + \Gamma M_J/(N+1) \ , \tag{8}$$

$$\langle F_2|H|F_2\rangle = E_2 + \Gamma M_J/[N(N+1)]\,, \tag{9}$$

$$\langle F_3|H|F_3\rangle = E_3 - \Gamma M_J/N\,, \tag{10}$$

$$\langle F_1|H|F_2\rangle = [\Gamma/(N+1)][N(N+M_J+1) \times (N-M_J+1)/(2N+1)]^{1/2}\,, \tag{11}$$

$$\langle F_2|H|F_3\rangle = [\Gamma/N][(N+1) \times (N+M_J)(N-M_J)/(2N+1)]^{1/2}\,, \tag{12}$$

where $\Gamma = g_s \mu_B B$ and F_1, F_2, and F_3 denote the three spin components of a given $N_{K_a K_c}$ level, with $J = N+1$, N, and $N-1$ and zero field energies E_1, E_2, and E_3, respectively. The resulting matrices, which are 3×3 or smaller, were diagonalized and the results plotted out using a desk-top calculator and plotter in a way that facilitated quick comparisons with the experimental spectra. This diagram was usually sufficient to assign the J and M_J quantum numbers to the components of the LMR spectra. The final calculations used the "full Zeeman matrix" program described in the next paragraph to calculate the predicted fields and relative intensities in order to confirm the assignments and resolve ambiguities.

The assigned data were then used to refine the molecular parameters appearing in the Hamiltonian by least-squares fitting. Preliminary fits used a program which treated the zero field problem exactly but retained only those matrix elements of the electron spin Zeeman Hamiltonian which are diagonal in the quantum numbers $N_{K_a K_c}$, as in the Zeeman plotting calculation. This approximation is an excellent one for CH_2 because the rotational levels are widely separated and because the first excited triplet electronic state is at very high energy, leading to small anisotropic Zeeman terms. The final fit was performed using a program[33,34] which set up the full Zeeman matrix in a parity conserving symmetric top basis set truncated so as to include all basis states up to and including $N' = N \pm 2$ and $K' = K \pm 4$; such restrictions were found empirically to introduce no significant errors. The approximate Zeeman calculation used in the preliminary analysis was found to introduce errors of 7 MHz or less when compared to this full calculation. The main fit was to the complete set of FIR LMR data together with the microwave frequencies[27] for the strongest ($\Delta J = \Delta N$) components of the 4_{04}–3_{13} transition; in this fit, the nuclear hyperfine structure was suppressed. Finally, the parameters obtained in the main fit were kept fixed, and the appropriate subset of the data for the *ortho*-CH_2 transitions (those involving levels with total nuclear spin $I = 1$) were fitted to determine the hyperfine parameters.

TABLE I. Far infrared laser lines used to observe LMR spectra of CH_2.

Lasing gas	Laser wavelength (μm)	Laser wave number (cm^{-1})	CH_2 transition ($N_{K_a K_c}$)
CH_2CHBr	680.5	14.694 182[c]	$2_{12} \leftarrow 3_{03}$
CD_2F_2	500.6	19.976 943[d]	$5_{05} \leftarrow 4_{14}$
CD_2F_2	317.0	31.540 569[d]	$1_{11} \leftarrow 2_{02}$
CH_3OH	163.0	61.337 076[e]	$2_{11} \leftarrow 2_{02}$ [a,b]
CH_2F_2	158.5	63.086 120[f]	$3_{12} \leftarrow 3_{03}$ [b]
			$1_{10} \leftarrow 1_{01}$
			$2_{11} \leftarrow 2_{02}$
$^{13}CH_3OH$	157.9	63.319 802[g]	$1_{10} \leftarrow 1_{01}$
CH_2DOH	150.8	66.305 835[h]	$2_{11} \leftarrow 2_{02}$
CD_2F_2	149.5	66.905 731[i]	$3_{12} \leftarrow 3_{03}$
$^{13}CH_3OH$	149.3	66.991 682[g]	$2_{11} \leftarrow 2_{02}$
			$3_{12} \leftarrow 3_{03}$
CD_3OH	144.1	69.387 647[j]	$4_{13} \leftarrow 4_{04}$
CD_3OH	128.0	78.104 379[j]	$1_{11} \leftarrow 0_{00}$
			$6_{15} \leftarrow 6_{06}$
CH_2DOH	108.8	91.896 764[h]	$2_{12} \leftarrow 1_{01}$
CH_2DOH	102.0	98.016 646[h]	$3_{22} \leftarrow 4_{13}$
			$4_{22} \leftarrow 5_{15}$
CH_3OH	63.4	157.804 522[e]	$5_{23} \leftarrow 5_{14}$
$^{13}CH_3OH$	63.1	158.487 690[g]	$5_{23} \leftarrow 5_{14}$

[a] Measurements of Mucha *et al.* (Ref. 23).
[b] Rotational transitions within the (100) excited vibrational state of CH_2; all other CH_2 transitions are within the (000) ground vibrational state.
[c] S. F. Dyubko, N. M. Efimenko, V. A. Svich, and L. D. Fesenko, Sov. J. Quantum Electron. **6**, 600 (1976).
[d] E. C. C. Vasconcellos, F. R. Petersen, and K. M. Evenson, Int. J. IR and Mm Waves **2**, 705 (1981).
[e] F. R. Peterson, K. M. Evenson, D. A. Jennings, and A. Scalabrin, IEEE J. Quantum Electron. QE-16, 319 (1980).
[f] F. R. Petersen, A. Scalabrin, and K. M. Evenson, Int. J. IR and Mm Waves **1**, 111 (1980).
[g] F. R. Petersen, D. A. Jennings, K. M. Evenson, and J. O. Henningsen (in preparation).
[h] A. Scalabrin, F. R. Petersen, K. M. Evenson, and D. A. Jennings, Int. J. IR and Mm Waves **1**, 117 (1980).
[i] The frequency of this new line pumped with the 10 R(18) line of the CO_2 laser was measured by Dr. F. R. Petersen at Natl. Bur. Stand., Boulder, Colorado. The 150.4 μm line previously reported to be pumped by this CO_2 line is actually pumped by 10 R(20).
[j] R. J. Saykally, K. M. Evenson, D. A. Jennings, and F. R. Petersen (in preparation).

IV. RESULTS

A. Introduction

We have observed and assigned 13 rotational transitions within the ground vibronic state $\tilde{X}\,^3B_1(000)$ of the methylene radical. Figure 2 shows the lower rotational energy levels of CH_2 and the observed LMR transitions, and Table I summarizes the laser lines used for the observations. Several CH_2 transitions were detected using two laser lines, and one of the strongest transitions $2_{11} - 2_{02}$ has components which were observed with three laser lines up to almost 4 cm^{-1} apart.

In contrast to the situation encountered in the analysis of the CH_2^- photoelectron spectrum[21] there is no doubt that, except where explicitly indicated, the observed transitions are within the zero point vibrational state of the molecule. The strongest support for this statement probably lies in the overall consistancy of the theoretical and mathematical interpretation of all the results. Near quantitative agreement with the earliest semirigid bender calculations[24,25] and more recent nonrigid bender fits of the entire data set are particularly convincing. These latter calculations allow accurate predictions of the spectra of the various isotopic modifications of the molecule and agreement between them

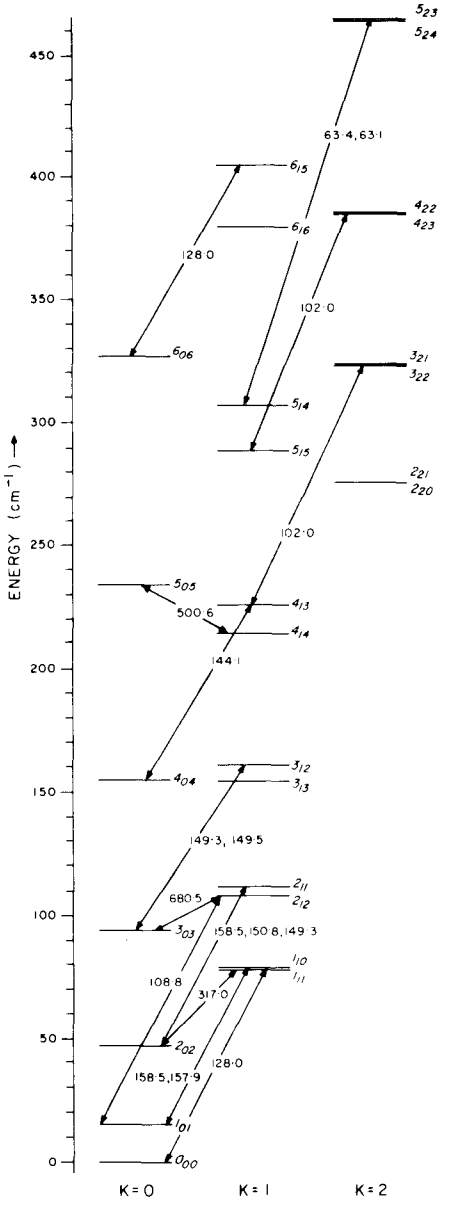

FIG. 2. Calculated rotational energy levels for CH_2. The arrows and associated numbers indicate the CH_2 transitions that were observed in this study (see Table II) and the wavelengths (in μm) of the laser lines used for the observations.

and very recently obtained spectra of $^{13}CH_2$ and CD_2[36] provides additional confirmation of the analysis.

Our work on CH_2 is the first observation of the spectrum of a polyatomic radical in a triplet state by LMR. In general, each rotational level, denoted by $N_{K_a K_c}$, is split into three fine structure components which are labeled F_1, F_2, and F_3 as $J=N+1$, N, and $N-1$, respectively. This splitting is typically of the order of 0.5 cm^{-1} in the levels observed, and hence a single rotational transition appears as several fine structure components spread over about 1 cm^{-1}. In the absence of an external magnetic field, the three components having $\Delta J=\Delta N$ are the strongest, but as a field is applied the Zeeman components fan out and transitions with nominal quantum number changes $\Delta J=\Delta N\pm1$ and $\Delta N\pm2$ are also likely to be observed. Thus, there is a good chance of detecting an LMR spectrum when there is a reasonably close coincidence in zero field between the laser and a CH_2 line.

An example of the observed CH_2 spectra is shown in Fig. 3. The upper trace was obtained with the electric vector of the laser radiation parallel to the applied magnetic field direction ($\Delta M_J=0$ selection rule) and the lower trace with it perpendicular ($\Delta M_J=\pm1$). Each was obtained using the 144.1 μm laser line of CD_3OH, and the observed resonances are Zeeman components of the $4_{13}-4_{04}$ rotational transition. This transition involves *ortho*-CH_2 ($I=1$) levels, and hence the resonances are all hyperfine triplets (though this is not always resolved). The effect of a magnetic field on the 4_{13} and 4_{04} energy levels is shown in Fig. 4, and the resulting behavior of the transition itself is plotted in Fig. 5. In this diagram (Fig. 5), the LMR lines are predicted at the fields where the vertical line (indicating the laser frequency) is crossed by the frequency vs field curve of the given CH_2 transition. This sort of diagram was a primary tool for the detailed assignment of the spectra. No information on the intensities of the LMR lines is given in these plots, but separate intensity calculations were also made to confirm our assignments. A strong single LMR line belonging to the $3_{12}-3_{03}$ transition is illustrated in Fig. 6; these are *para*-CH_2 levels, and so there is no hyperfine splitting. A saturation resonance

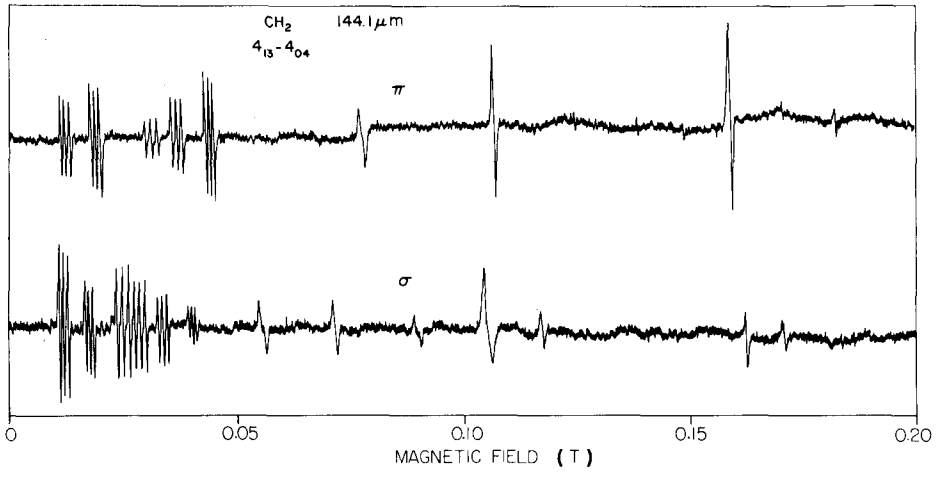

FIG. 3. Laser magnetic resonance spectrum of CH_2 obtained with the 144.1 μm (69.38765 cm^{-1}) laser line of CD_3OH in π and σ polarizations. The resonances observed here are various Zeeman components of the $4_{13}-4_{04}$ rotational transition, and for many of them the triplet hyperfine structure is resolved.

(inverse Lamb dip) is clearly evident at line center (Fig. 6).

B. Determination of molecular parameters

The measured LMR transitions that were assigned to the ground vibrational state of CH_2 are listed in Table II. Only the field position of the central component of the nuclear hyperfine triplet is listed here in cases where hyperfine splitting was resolved; hyperfine effects are considered separately in Sec. IV D below. The data in Table II were fitted by least squares to the parameters appearing in the effective Hamiltonian Eqs. (1)–(5) and (7). The resulting parameters are given in Table III, and the quality of the fit may be judged from the obs-calc columns in Table II. In the fit, the electron spin g factors were constrained at the values predicted by Curl's relation[37] (which has been shown to be quite satisfactory for a light molecule such as CH_2). The rotational g factors were constrained at values predicted by the relation[34] $g_r^{\alpha\alpha} = -|\epsilon_{\alpha\alpha}|/\zeta$, where $\epsilon_{\alpha\alpha}$ is the appropriate spin-rotation parameter and ζ is an effective spin-orbit parameter (in this case, that of the carbon atom $\zeta = 28$ cm^{-1}).

The results of the fit are highly satisfactory in that almost all the data are fitted to within their experimental precision. The final set of parameters fit were all well determined as can be judged from the statistical

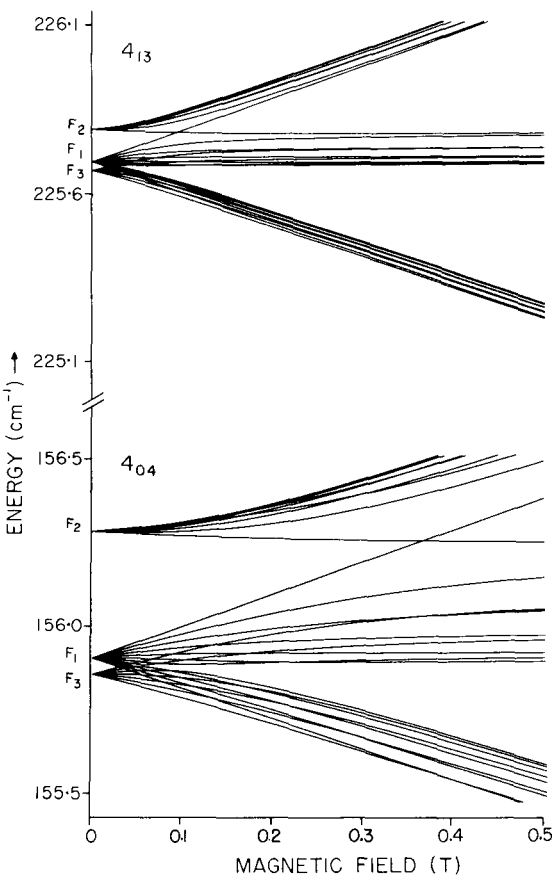

FIG. 4. Calculated Zeeman splitting patterns for the 4_{13} and 4_{04} rotational levels of CH_2. Transitions between these two levels give rise to the spectrum of Fig. 3.

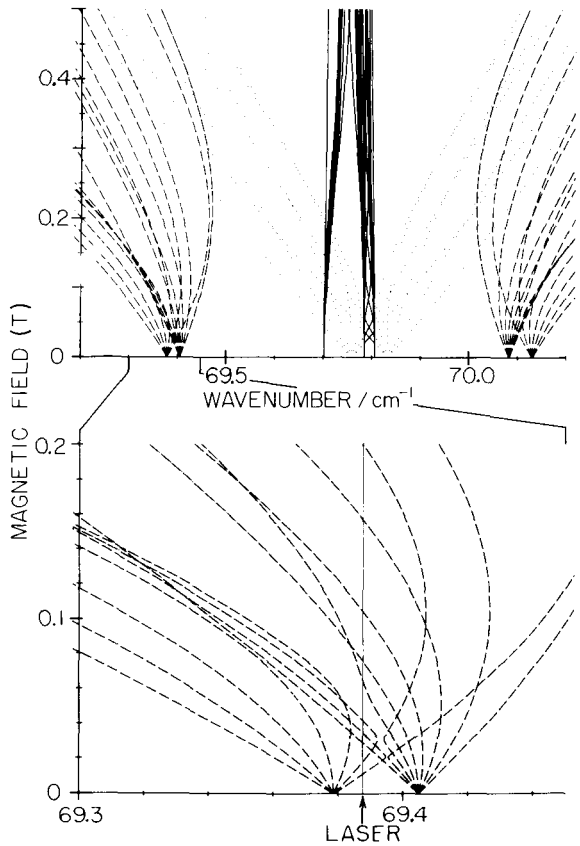

FIG. 5. Calculated Zeeman effect spectrum diagram illustrating the 4_{13}–4_{04} transition in π polarization (upper trace of Fig. 3). The upper part of this figure shows the entire 4_{13}–4_{04} transition, and the lower part shown an enlargement of the section responsible for the observed spectrum of Fig. 2. Each crossing of the laser frequency by one of the dashed lines in lower section represents a possible LMR transition. Zeeman components with $\Delta J = \Delta N$ are solid lines, those with $\Delta J = \Delta N \pm 1$ are dashed, and those with $\Delta J = \Delta N \pm 2$ are dotted.

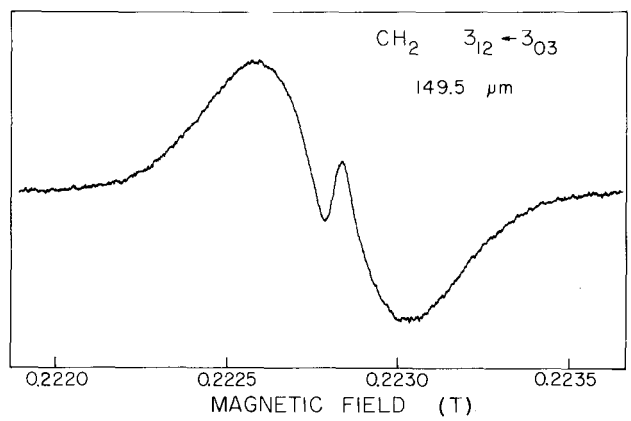

FIG. 6. A portion of the LMR spectrum of CH_2 recorded in perpendicular (σ) polarization with the 149.5 μm (66.9051 cm^{-1}) laser line of CD_2F_2. The line shown here is one Zeeman component of the $3_{12} \leftarrow 3_{03}$ rotational transition (see Table II) and it is one of the strongest CH_2 transitions observed in this work. A saturation resonance (inverse Lamb dip) is clearly evident at the line center; the sample pressure was reduced to 20 Pa (150 mTorr) for this recording to permit the clear observation of the saturation feature.

TABLE II. Observed transitions in the ground vibrational state of CH_2.

Laser line (cm^{-1})[a]	Resonant field (T)	Assignment[b] $N_{K_aK_c}$	J	M_J	Obs.−Calc. (MHz)	(G)[c]	TR[d]	Int.[e]
2.28079[f,g]		4 0 4 ← 3 1 3	5 ← 4		−0.2			
2.35761[f,g]		4 0 4 ← 3 1 3	4 ← 3		0.6			
2.30199[f,h]		4 0 4 ← 3 1 3	3 ← 2		−0.7			
14.6942	0.12242	2 1 2 ← 3 0 3	2 ← 3	1 ← 1	1.1	−2.0	0.54	88
14.6942	0.14316	2 1 2 ← 3 0 3	2 ← 3	0 ← 0	1.0	−2.0	0.52	86
14.6942	0.14835	2 1 2 ← 3 0 3	2 ← 3	2 ← 2	1.3	−3.6	0.35	67
14.6942	0.25944	2 1 2 ← 3 0 3	2 ← 3	−1 ← −1	−1.0	+3.3	0.31	58
14.6942	0.66147	2 1 2 ← 3 0 3	3 ← 3	3 ← 3	−4.3	+16.1	0.27	49
14.6942	0.09213	2 1 2 ← 3 0 3	2 ← 3	1 ← 0	2.2	−3.2	0.66	42
14.6942	0.09467	2 1 2 ← 3 0 3	2 ← 3	0 ← −1	2.2	−2.7	0.80	76
14.6942	0.11721	2 1 2 ← 3 0 3	2 ← 3	−1 ← −2	1.5	−1.8	0.82	118
14.6942	0.12659	2 1 2 ← 3 0 3	2 ← 3	2 ← 3	1.8	−2.8	0.63	127
14.6942	0.13065	2 1 2 ← 3 0 3	2 ← 3	2 ← 1	1.7	−6.4	0.26	19
14.6942	0.13341	2 1 2 ← 3 0 3	2 ← 3	1 ← 2	1.3	−2.2	0.62	74
14.6942	0.19340	2 1 2 ← 3 0 3	2 ← 3	0 ← 1	0.2	−0.5	0.40	36
19.9769	0.26907	5 0 5 ← 4 1 4	5 ← 5	5 ← 5	−2.7	−1.8	−1.45	19
19.9769	0.42713	5 0 5 ← 4 1 4	5 ← 4	−4 ← −4	3.7	−1.7	2.23	8
19.9769	0.31837	5 0 5 ← 4 1 4	6 ← 3	−2 ← −1	0.1	0.0	2.53	2
19.9769	0.32268	5 0 5 ← 4 1 4	6 ← 3	0 ← 1	−1.7	+0.7	2.33	1
19.9769	0.34964	5 0 5 ← 4 1 4	6 ← 3	−1 ← 0	−1.6	+0.7	2.44	3
19.9769	0.35200	5 0 5 ← 4 1 4	5 ← 5	4 ← 5	−1.5	−2.0	−0.74	3
31.5406	0.02974	1 1 1 ← 2 0 2	2 ← 3	−2 ← −2	−3.1	−3.7	−0.84	230
31.5406	0.03804	1 1 1 ← 2 0 2	1 ← 1	−1 ← −1	10.0	+3.3	−2.98	149
31.5406	0.36177	1 1 1 ← 2 0 2	2 ← 3	−1 ← −1	−2.7	−6.0	−0.45	276
31.5406	0.01429	1 1 1 ← 2 0 2	2 ← 3	−2 ← −1	−5.0	−2.8	−1.79	46
31.5406	0.02134	1 1 1 ← 2 0 2	2 ← 3	−1 ← 0	−3.8	−3.6	−1.06	137
31.5406	0.07285	1 1 1 ← 2 0 2	1 ← 1	−1 ← 0	12.5	+7.9	−1.59	174
31.5406	0.33364	1 1 1 ← 2 0 2	2 ← 3	−1 ← 0	2.9	−18.4	0.16	118
63.0861	0.36660	1 1 0 ← 1 0 1	1 ← 1	0 ← 0	−9.6	−2.1	−4.61	88
63.0861	0.61436	1 1 0 ← 1 0 1	1 ← 1	1 ← 1	−10.3	−4.0	−2.56	432
63.0861	0.61436	1 1 0 ← 1 0 1	1 ← 1	−1 ← −1	−12.3	−4.8	−2.56	144
63.0861	0.95212	1 1 0 ← 1 0 1	2 ← 1	0 ← 0	7.3	+2.8	−2.60	93
63.0861	1.06176	1 1 0 ← 1 0 1	1 ← 2	0 ← 0	−1.4	−0.5	−2.65	256
63.0861	1.04649	2 1 1 ← 2 0 2	1 ← 2	1 ← 1	6.5	+1.2	−5.53	70
63.0861	1.08416	2 1 1 ← 2 0 2	1 ← 2	0 ← 0	1.6	+0.3	−5.52	49
63.0861	0.31601	1 1 0 ← 1 0 1	1 ← 1	0 ← 1	−11.3	−2.4	−4.75	562
63.0861	0.32880	1 1 0 ← 1 0 1	1 ← 1	−1 ← 0	−9.7	−2.1	−4.66	985
63.0861	0.69763	1 1 0 ← 1 0 1	1 ← 1	0 ← −1	−7.8	−3.1	−2.54	106
63.0861	0.73039	1 1 0 ← 1 0 1	2 ← 1	−2 ← −1	2.8	+1.0	−2.67	331
63.0861	0.76113	1 1 0 ← 1 0 1	2 ← 1	−1 ← 0	−4.2	−1.6	−2.60	68
63.3198	0.20038	1 1 0 ← 1 0 1	1 ← 1	0 ← 0	−18.2	−5.0	−3.67	117
63.3198	0.32300	1 1 0 ← 1 0 1	1 ← 1	1 ← 1	−16.9	−7.8	−2.17	1042
63.3198	0.32300	1 1 0 ← 1 0 1	1 ← 1	−1 ← −1	−18.0	−8.3	−2.17	411
63.3198	0.67423	1 1 0 ← 1 0 1	2 ← 1	0 ← 0	−1.9	−0.8	−2.43	200
63.3198	0.79094	1 1 0 ← 1 0 1	1 ← 2	0 ← 0	−7.1	−2.8	−2.51	482
63.3198	0.15570	1 1 0 ← 1 0 1	1 ← 1	0 ← 1	−19.4	−5.0	−3.85	1188
63.3198	0.16400	1 1 0 ← 1 0 1	1 ← 1	−1 ← 0	−19.6	−5.3	−3.70	1751
66.3058	0.52112	2 1 1 ← 2 0 2	2 ← 1	1 ← 1	−7.8	+1.5	5.29	42
66.3058	0.58890	2 1 1 ← 2 0 2	2 ← 1	0 ← 0	−6.5	+1.2	5.29	175
66.3058	0.63578	2 1 1 ← 2 0 2	2 ← 1	−1 ← −1	2.7	−0.5	5.40	214
66.3058	1.13725	2 1 1 ← 2 0 2	2 ← 3	−1 ← −1	0.3	−0.1	2.74	125
66.3058	1.15916	2 1 1 ← 2 0 2	2 ← 3	−2 ← −2	−11.9	+4.3	2.74	95
66.3058	0.52621	2 1 1 ← 2 0 2	2 ← 1	0 ← 1	10.4	−2.0	5.29	15
66.3058	0.53081	2 1 1 ← 2 0 2	2 ← 1	2 ← 1	−3.5	+0.7	5.27	190
66.3058	0.58340	2 1 1 ← 2 0 2	2 ← 1	1 ← 0	−5.2	+1.0	5.28	164
66.3058	0.61015	2 1 1 ← 2 0 2	2 ← 1	−1 ← 0	−0.3	−0.0	5.29	27
66.3508	0.61179	2 1 1 ← 2 0 2	2 ← 3	−1 ← −2	3.1	−0.6	5.41	15
66.3058	0.61487	2 1 1 ← 2 0 2	2 ← 1	0 ← −1	−3.6	+0.7	5.40	20
66.3058	1.05405	2 1 1 ← 2 0 2	3 ← 1	2 ← 1	−8.0	+2.9	2.73	86
66.3058	1.05776	2 1 1 ← 2 0 2	2 ← 3	−2 ← −3	−9.0	+3.2	2.79	19
66.3058	1.09407	2 1 1 ← 2 0 2	2 ← 3	0 ← −1	−4.4	+1.6	2.74	75
66.3058	1.26672	2 1 1 ← 2 0 2	3 ← 3	−1 ← −2	7.5	−2.7	2.76	36
66.3058	1.27472	2 1 1 ← 2 0 2	3 ← 1	−1 ← 0	1.3	−0.5	2.75	56
66.3058	1.31666	2 1 1 ← 2 0 2	2 ← 3	1 ← 2	−14.9	+5.4	2.74	94
66.3058	1.34667	2 1 1 ← 2 0 2	3 ← 1	0 ← −1	6.3	−2.3	2.76	34

TABLE II (*Continued*)

Laser line (cm^{-1})[a]	Resonant field (T)	Assignment[b] $N_{K_a K_c}$	J	M_J	Obs. − Calc. (MHz)	(G)[c]	TR[d]	Int.[e]
66.3058	1.39838	2 1 1 ← 2 0 2	3 ← 3	3 ← 2	2.6	−1.0	2.75	88
66.9057	0.22281	3 1 2 ← 3 0 3	4 ← 3	4 ← 3	3.9	−3.0	1.29	1529
66.9057	0.30330	3 1 2 ← 3 0 3	2 ← 4	−1 ← −2	−8.6	−2.7	−3.19	163
66.9057	0.32469	3 1 2 ← 3 0 3	2 ← 4	0 ← 1	−4.9	−2.0	−2.45	226
66.9057	0.32542	3 1 2 ← 3 0 3	3 ← 3	−3 ← −2	−28.5	−14.6	−1.96	760
66.9057	0.35868	3 1 2 ← 3 0 3	2 ← 4	−2 ← −1	−4.7	−1.7	−2.75	95
66.9057	0.37097	3 1 2 ← 3 0 3	2 ← 4	0 ← −1	−5.2	−1.9	−2.73	171
66.9057	0.38887	3 1 2 ← 3 0 3	2 ← 4	−1 ← 0	−8.1	−3.2	−2.55	403
66.9057	0.41505	3 1 2 ← 3 0 3	4 ← 4	3 ← 4	3.3	+1.3	−2.48	335
66.9917	0.16826	3 1 2 ← 3 0 3	2 ← 4	1 ← 1	6.0	+2.8	−2.14	93
66.9917	0.27169	3 1 2 ← 3 0 3	2 ← 4	0 ← 0	−2.1	−0.9	−2.23	51
66.9917	0.16360	3 1 2 ← 3 0 3	3 ← 3	−3 ← −2	−27.3	−23.5	−1.16	1453
66.9917	0.21491	3 1 2 ← 3 0 3	2 ← 4	0 ← 1	−0.1	0.0	−2.19	267
66.9917	0.22417	3 1 2 ← 3 0 3	2 ← 4	−1 ← −2	−3.9	−1.2	−3.30	196
66.9917	0.26406	3 1 2 ← 3 0 3	2 ← 4	−2 ← −1	−4.0	−1.5	−2.69	233
66.9917	0.27499	3 1 2 ← 3 0 3	2 ← 4	0 ← −1	−3.2	−1.2	−2.62	245
66.9917	0.28390	3 1 2 ← 3 0 3	2 ← 4	−1 ← 0	−5.2	−2.2	−2.33	817
66.9917	0.30578	3 1 2 ← 3 0 3	4 ← 4	3 ← 4	−7.2	−3.2	−2.23	592
66.9917	0.90125	2 1 1 ← 2 0 2	2 ← 1	1 ← 1	32.8	−6.0	5.47	17
66.9917	0.96810	2 1 1 ← 2 0 2	2 ← 1	0 ← 0	33.5	−6.1	5.49	70
66.9917	1.01094	2 1 1 ← 2 0 2	2 ← 1	−1 ← −1	40.8	−7.4	5.52	86
66.9917	1.88101	2 1 1 ← 2 0 2	2 ← 3	−1 ← −1	15.1	−5.4	2.78	47
66.9917	1.90278	2 1 1 ← 2 0 2	2 ← 3	−2 ← −2	0.7	−0.3	2.78	41
66.9917	0.91148	2 1 1 ← 2 0 2	2 ← 1	2 ← 1	38.5	−7.0	5.47	77
66.9917	0.96267	2 1 1 ← 2 0 2	2 ← 1	1 ← 0	34.4	−6.3	5.49	64
69.3876	0.01056	4 1 3 ← 4 0 4	3 ← 4	−3 ← −3	15.1	−6.3	2.41	114
69.3876	0.01721	4 1 3 ← 4 0 4	3 ← 4	−2 ← −2	11.7	−8.5	1.38	202
69.3876	0.02943	4 1 3 ← 4 0 4	5 ← 4	−4 ← −4	3.2	+1.7	−1.82	57
69.3876	0.03508	4 1 3 ← 4 0 4	3 ← 4	−3 ← −3	3.3	+2.0	−1.67	114
69.3876	0.04232	4 1 3 ← 4 0 4	3 ← 4	−2 ← −2	4.2	+2.7	−1.54	205
69.3876	0.07600	4 1 3 ← 4 0 4	5 ← 4	0 ← 0	4.5	+3.8	−1.19	80
69.3876	0.10493	4 1 3 ← 4 0 4	5 ← 4	1 ← 1	4.3	+3.5	−1.23	116
69.3876	0.15719	4 1 3 ← 4 0 4	5 ← 4	2 ← 2	1.9	+1.5	−1.27	144
69.3876	0.20042	4 1 3 ← 4 0 4	5 ← 4	−2 ← −2	5.4	+4.8	−1.13	47
69.3876	0.25971	4 1 3 ← 4 0 4	5 ← 4	3 ← 3	−0.8	−0.6	−1.39	189
69.3876	0.31811	4 1 3 ← 4 0 4	3 ← 5	3 ← 3	4.6	+1.5	−3.15	22
69.3876	0.42274	4 1 3 ← 4 0 4	3 ← 5	2 ← 2	0.6	+0.2	−2.69	31
69.3876	0.46016	4 1 3 ← 4 0 4	5 ← 4	4 ← 4	−11.8	−6.6	−1.79	276
69.3876	0.00989	4 1 3 ← 4 0 4	3 ← 4	−3 ← −4	15.1	−5.8	2.60	478
69.3876	0.01536	4 1 3 ← 4 0 4	3 ← 4	−2 ← −3	12.0	−7.5	1.60	366
69.3876	0.02272	4 1 3 ← 4 0 4	5 ← 4	−5 ← −4	2.5	+1.1	−2.29	334
69.3876	0.02642	4 1 3 ← 4 0 4	5 ← 4	−4 ← −3	2.5	+1.2	−2.07	276
69.3876	0.03139	4 1 3 ← 4 0 4	3 ← 4	−3 ← −2	2.9	+1.6	−1.88	217
69.3876	0.03781	4 1 3 ← 4 0 4	3 ← 4	−2 ← −1	4.1	+2.5	−1.63	127
69.3876	0.05290	4 1 3 ← 4 0 4	5 ← 4	−1 ← 0	2.5	+2.5	−0.98	205
69.3876	0.06923	4 1 3 ← 4 0 4	5 ← 4	0 ← 1	5.0	+4.2	−1.21	154
69.3876	0.08731	4 1 3 ← 4 0 4	5 ← 4	0 ← −1	4.9	+4.4	−1.11	117
69.3876	0.10122	4 1 3 ← 4 0 4	5 ← 4	−1 ← −2	5.6	+10.9	−0.52	328
69.3876	0.10122	4 1 3 ← 4 0 4	5 ← 4	1 ← 2	5.7	+4.9	−1.16	121
69.3876	0.11362	4 1 3 ← 4 0 4	5 ← 4	1 ← 0	4.9	+3.9	−1.27	99
69.3876	0.15832	4 1 3 ← 4 0 4	5 ← 4	2 ← 1	1.9	+1.4	−1.35	100
69.3876	0.16666	4 1 3 ← 4 0 4	5 ← 4	2 ← 3	1.9	+1.6	−1.15	96
69.3876	0.23903	4 1 3 ← 4 0 4	5 ← 4	3 ← 2	0.2	+0.2	−1.46	95
69.3876	0.28237	4 1 3 ← 4 0 4	5 ← 4	−2 ← −3	5.0	+3.9	−1.30	423
69.3876	0.31630	4 1 3 ← 4 0 4	5 ← 4	3 ← 4	−2.8	−2.1	−1.35	47
69.3876	0.39120	4 1 3 ← 4 0 4	5 ← 4	4 ← 3	−7.3	−4.3	−1.72	66
69.3876	0.39467	4 1 3 ← 4 0 4	3 ← 5	−2 ← −3	−5.6	−1.8	−3.08	27
69.3876	0.46113	4 1 3 ← 4 0 4	3 ← 5	1 ← 2	−2.9	−1.1	−2.68	24
69.3876	0.50413	4 1 3 ← 4 0 4	3 ← 5	−1 ← −2	−6.2	−2.2	−2.78	63
69.3876	0.54491	4 1 3 ← 4 0 4	3 ← 5	0 ← 1	−7.5	−2.8	−2.65	77
69.3876	0.54491	4 1 3 ← 4 0 4	3 ← 5	−2 ← −1	−6.4	−2.4	−2.70	25
69.3876	0.55993	4 1 3 ← 4 0 4	3 ← 5	0 ← −1	−6.0	−2.2	−2.72	54
69.3876	0.57662	4 1 3 ← 4 0 4	3 ← 5	−1 ← 0	−9.4	−3.5	−2.68	77
69.3876	0.59691	4 1 3 ← 4 0 4	4 ← 4	−4 ← −3	−28.4	−11.2	−2.52	186
69.3876	0.64595	4 1 3 ← 4 0 4	5 ← 5	4 ← 5	−15.6	−5.9	−2.62	119

TABLE II (*Continued*)

Laser line (cm^{-1})[a]	Resonant field (T)	Assignment[b] $N_{K_aK_c}$	Assignment[b] J	Assignment[b] M_J	Obs.–Calc. (MHz)	Obs.–Calc. (G)[c]	TR[d]	Int.[e]
78.1044	0.15764	1 1 1 ← 0 0 0	1 ← 1	1 ← 1	8.8	+3.8	−2.33	364
78.1044	0.20474	1 1 1 ← 0 0 0	1 ← 1	0 ← 0	14.5	+3.3	−4.41	3228
78.1044	0.08649	1 1 1 ← 0 0 0	1 ← 1	0 ← 1	15.2	+6.2	−2.45	1978
78.1044	0.15769	1 1 1 ← 0 0 0	1 ← 1	−1 ← 0	15.9	+6.5	−2.45	1978
78.1044	0.30800	1 1 1 ← 0 0 0	2 ← 1	0 ← 1	−7.8	−3.1	−2.55	1504
78.1044	0.37343	6 1 5 ← 6 0 6	6 ← 5	1 ← 1	−0.4	+0.1	4.94	21
78.1044	0.37734	6 1 5 ← 6 0 6	6 ← 5	−3 ← −3	−1.3	+0.3	4.84	21
78.1044	0.38026	6 1 5 ← 6 0 6	6 ← 5	−2 ← −2	2.8	−0.6	4.89	26
78.1044	0.38074	6 1 5 ← 6 0 6	6 ← 5	0 ← 0	−0.6	+0.1	4.97	26
78.1044	0.38262	6 1 5 ← 6 0 6	6 ← 5	−1 ← −1	−1.1	+0.2	4.94	28
91.8968	0.37409	2 1 2 ← 1 0 1	1 ← 1	1 ← 1	−12.3	−2.4	−5.04	351
91.8968	0.46320	2 1 2 ← 1 0 1	1 ← 1	0 ← 0	−5.2	−1.1	−4.97	225
91.8968	0.80873	2 1 2 ← 1 0 1	3 ← 1	1 ← 1	−0.4	−0.1	−2.71	139
91.8968	0.86559	2 1 2 ← 1 0 1	1 ← 2	1 ← 1	−3.7	−1.3	−2.86	69
91.8968	0.87783	2 1 2 ← 1 0 1	3 ← 1	0 ← 0	−3.2	−1.2	−2.61	98
91.8968	0.88692	2 1 2 ← 1 0 1	1 ← 1	−1 ← −1	−0.0	−0.0	−2.68	244
91.8968	1.13688	2 1 2 ← 1 0 1	3 ← 2	2 ← 2	7.5	+2.7	−2.78	86
91.8968	1.22014	2 1 2 ← 1 0 1	1 ← 2	0 ← 0	9.5	+3.5	−2.72	160
91.8968	0.41106	2 1 2 ← 1 0 1	1 ← 1	0 ← 1	−6.4	−1.2	−5.10	281
91.8968	0.42501	2 1 2 ← 1 0 1	1 ← 1	1 ← 0	−13.3	−2.7	−4.89	1338
91.8968	0.75584	2 1 2 ← 1 0 1	3 ← 1	0 ← 1	−5.9	−2.2	−2.68	207
91.8968	0.86588	2 1 2 ← 1 0 1	1 ← 1	0 ← −1	1.3	+0.5	−2.66	413
91.8968	0.93112	2 1 2 ← 1 0 1	3 ← 1	2 ← 1	5.0	+1.9	−2.68	163
91.8968	0.93163	2 1 2 ← 1 0 1	3 ← 1	1 ← 0	2.7	+1.0	−2.64	137
91.8968	1.15177	2 1 2 ← 1 0 1	1 ← 2	1 ← 0	−0.2	−0.1	−2.70	312
91.8968	1.23999	2 1 2 ← 1 0 1	1 ← 2	−1 ← 0	7.9	+2.9	−2.72	160
98.0166	0.11038	3 2 2 ← 4 1 3	2 ← 3	2 ← 2	−1.5	+0.3	4.80	31
98.0166	0.12188	3 2 2 ← 4 1 3	2 ← 3	1 ← 1	−1.2	+0.3	4.49	67
98.0166	0.13345	3 2 2 ← 4 1 3	2 ← 3	0 ← 0	0.2	−0.0	4.42	97
98.0166	0.13469	3 2 2 ← 4 1 3	2 ← 3	−1 ← −1	−0.3	+0.1	4.59	56
98.0166	0.19086	3 2 2 ← 4 1 3	2 ← 5	−1 ← −1	−5.0	+1.9	2.69	31
98.0166	0.20765	3 2 2 ← 4 1 3	4 ← 3	3 ← 3	−4.9	+1.9	2.56	15
98.0166	0.21239	3 2 2 ← 4 1 3	2 ← 5	1 ← 1	−0.7	+0.2	2.82	17
98.0166	0.22545	3 2 2 ← 4 1 3	2 ← 5	−2 ← −2	−3.7	+1.5	2.49	44
98.0166	0.24488	3 2 2 ← 4 1 3	3 ← 3	2 ← 2	−4.0	+1.6	2.40	38
98.0166	0.25265	3 2 2 ← 4 1 3	2 ← 5	2 ← 2	0.4	−0.2	2.64	44
98.0166	0.26386	3 2 2 ← 4 1 3	3 ← 3	−3 ← −3	2.2	−0.9	2.47	18
98.0166	0.28375	3 2 2 ← 4 1 3	3 ← 3	1 ← 1	−0.1	−0.0	2.39	30
98.0166	0.29459	3 2 2 ← 4 1 3	3 ← 3	−2 ← −2	4.0	−1.7	2.44	24
98.0166	0.31330	3 2 2 ← 4 1 3	3 ← 5	3 ← 3	4.6	−1.9	2.44	57
98.0166	0.41026	3 2 2 ← 4 1 3	4 ← 5	4 ← 4	10.0	−4.3	2.31	40
98.0166	0.18110	4 2 2 ← 5 1 5	4 ← 4	4 ← 4	−5.4	+1.2	4.65	12
98.0166	0.18514	4 2 2 ← 5 1 5	4 ← 4	3 ← 3	−4.7	+1.0	4.64	15
98.0166	0.19545	4 2 2 ← 5 1 5	4 ← 4	2 ← 2	−3.7	+0.8	4.58	18
98.0166	0.20947	4 2 2 ← 5 1 5	4 ← 4	1 ← 1	−2.6	+0.6	4.55	20
98.0166	0.22297	4 2 2 ← 5 1 5	4 ← 4	0 ← 0	−1.5	+0.3	4.63	20
98.0166	0.22842	4 2 2 ← 5 1 5	4 ← 4	−1 ← −1	2.1	−0.4	4.68	14
98.0166	0.56673	4 2 2 ← 5 1 5	4 ← 6	4 ← 4	4.6	−1.8	2.51	16
98.0166	0.72635	4 2 2 ← 5 1 5	5 ← 6	5 ← 5	10.6	−4.1	2.57	16
157.8045	0.35502	5 2 3 ← 5 1 4	6 ← 5	4 ← 4	6.8	+1.4	−4.97	21
157.8045	0.35750	5 2 3 ← 5 1 4	6 ← 5	3 ← 3	3.7	+0.7	−5.06	36
157.8045	0.36364	5 2 3 ← 5 1 4	6 ← 5	2 ← 2	2.0	+0.4	−5.12	43
157.8045	0.37071	5 2 3 ← 5 1 4	6 ← 5	1 ← 1	0.5	+0.1	−5.18	42
157.8045	0.37653	5 2 3 ← 5 1 4	6 ← 5	0 ← 0	−5.2	−1.0	−5.20	34
157.8045	0.38035	5 2 3 ← 5 1 4	6 ← 5	−1 ← −1	−6.7	−1.3	−5.17	22
157.8045	0.38325	5 2 3 ← 5 1 4	6 ← 5	−2 ← −2	−5.3	−1.0	−5.10	12
157.8045	0.85131	5 2 3 ← 5 1 4	4 ← 5	4 ← 4	−3.8	−1.4	−2.66	28
157.8045	0.97727	5 2 3 ← 5 1 4	6 ← 5	5 ← 5	−23.4	−8.7	−2.69	35
158.4877	0.22402	5 2 3 ← 5 1 4	6 ← 6	0 ← 0	−14.3	−5.9	−2.44	0
158.4877	0.16586	5 2 3 ← 5 1 4	5 ← 5	−5 ← −4	11.1	+10.0	−1.11	720
158.4877	0.17935	5 2 3 ← 5 1 4	6 ← 6	−1 ← −2	4.8	+1.9	−2.50	103
158.4877	0.21083	5 2 3 ← 5 1 4	6 ← 6	0 ← 1	2.2	+0.9	−2.41	214
158.4877	0.21402	5 2 3 ← 5 1 4	6 ← 6	0 ← −1	8.4	−3.4	−2.45	150
158.4877	0.22107	5 2 3 ← 5 1 4	6 ← 6	−1 ← 0	2.2	−0.9	−2.40	163

TABLE II (*Continued*)

Laser line (cm^{-1})[a]	Resonant field (T)	Assignment[b] $N_{K_aK_c}$	J	M_J	Obs. − Calc. (MHz)	(G)[c]	TR[d]	Int.[e]
158.4877	0.28516	5 2 3 ← 5 1 4	6 ← 6	5 ← 6	−3.8	−1.8	−2.13	302
158.4877	0.40571	5 2 3 ← 5 1 4	6 ← 5	6 ← 5	21.0	−33.7	0.62	978

[a]See Table I.
[b]The assignment given for J is that with which the given M_J level correlates at zero field.
[c]1 G (Gauss) = 10^{-4} T (Tesla).
[d]Calculated tuning rate of the given transition in MHz/G.
[e]Calculated relative line intensity, including Boltmann factor for 300 K.
[f]Microwave measurements (Ref. 27) with hyperfine splittings removed.
[g]Transition given a relative weight of 400 in the fit (estimated error 0.1 MHz).
[h]Transition given a relative weight of 100 in the fit (estimated error 0.2 MHz).

uncertainties given in Table III and the fact that the only off-diagonal elements of the correlation matrix greater than 0.95 were those between $\frac{1}{2}(B+C)$ and Δ_N(0.969), Φ_{NK} and Δ_{NK}(0.976), and ϕ_N and δ_N(0.957). However, it was necessary to use 11 rotational and centrifugal distortion parameters to fit the 14 observed rotational transitions. This large number of parameters is indicative of a rather slow convergence of the effective centrifugal distortion Hamiltonian. Similar difficulties arise when fitting the spectra of other very light molecules such as H_2O and NH_2,[38] but the problem is especially severe in CH_2 because it is more nearly linear, and its bending motion is both very anharmonic and of large amplitude. Thus, the precise values of the parameters in Table III are not particularly significant: for example, if the parameter Φ_K is fixed at a value (0.130 cm^{-1}) determined from the positions of $K_a = 3$ levels calculated by the semirigid bender program,[25,26] the parameters A and Δ_K are considerably changed (to 73.577 and 2.641 cm^{-1}) from their values in Table III. As a consequence, it is not possible to use this effective Hamiltonian to reliably estimate the zero point geometrical structure for the molecule. Instead a more realistic model, explicitly allowing for the large amplitude bending motion is required. This problem is treated in the following papers.

In contrast to the rotational and centrifugal distortion parameters, those describing the spin–spin and spin-rotation interactions are quite unambiguously determined, and there is no need to make centrifugal distortion corrections to the spin parameters for the transitions analyzed here. The present values for the spin–spin parameters D and E are compared in Table IV with earlier values based on *ab initio* calculations and on matrix ESR experiments. In the ESR experiments, it is difficult to determine the true free molecule spin parameters because of the perturbing effects of the matrix on the observed spectra. In view of this difficulty, the agreement between our parameters and those from ESR (Table IV) is rather good. The *ab initio* calculations[13,14] are also fairly close to our values; however, it is interesting to note that the value calculated for D *omitting* spin-orbit contributions[14(a)] ($D = 0.781$ cm^{-1}) is considerably closer to our value, suggesting that these contributions may be smaller than expected.[14(b)] Such a conclusion is also suggested by a very recent calculation.[41] The calculated spin parameters of course refer to CH_2 in its equilibrium configuration, whereas our ex-

TABLE III. Molecular parameters for the ground $\tilde{X}\,^3B_1$ state of CH_2.[a]

	Parameter	Value	Unit
Rotation	A	73.057 75(11)	cm^{-1}
	B	8.415 172 (76)	cm^{-1}
	C	7.219 272 (45)	cm^{-1}
Centrifugal distortion	Δ_K	1.991 049 (47)	cm^{-1}
	Δ_{NK}	−0.019 660 (27)	cm^{-1}
	Δ_N	0.000 301 3(34)	cm^{-1}
	δ_N	$0.101\,2(12)\times10^{-3}$	cm^{-1}
	Φ_{KN}	−0.001 941 7(21)	cm^{-1}
	Φ_{NK}	$0.128\,1(86)\times10^{-4}$	cm^{-1}
	Φ_N	$0.251\,(59)\times10^{-6}$	cm^{-1}
	φ_N	$0.195\,(30)\times10^{-6}$	cm^{-1}
Spin–spin	D	0.778 42(14)	cm^{-1}
	E	0.039 906(38)	cm^{-1}
Spin–rotation	ϵ_{aa}	0.000 446(78)	cm^{-1}
	ϵ_{bb}	−0.005 148(18)	cm^{-1}
	ϵ_{cc}	−0.004 106 (27)	cm^{-1}
Hyperfine	a_{FC}	−20.26(51)	MHz
	T_{aa}	39.7(17)	MHz
	T_{bb}	−20.2(19)	MHz

[a]Parameters not appearing in this table were fixed at zero. In the Zeeman Hamiltonian, g factors were fixed (see the text) at the following values: $g_s^{aa} = 2.002\,315$; $g_s^{bb} = 2.002\,624$; $g_s^{cc} = 2.002\,604$; $g_r^{aa} = -0.000\,020$; $g_r^{bb} = -0.000\,257$; $g_b^{cc} = -0.000\,147$. The numbers in parentheses are one standard deviation of the least-squares fits in units of the last quoted digit.

TABLE IV. Comparison of present and previous values for spin–spin interaction parameters in CH_2.

	D/cm^{-1}	E/cm^{-1}
Present work (LMR)	0.778 4(1)	0.039 91(4)
Wasserman *et al.* (ESR)[a]	0.76(2)	0.052 (17)
Bicknell *et al.* (ESR)[b]	0.79	•••
Langhoff (*ab initio*)[c]	0.807	0.050

[a]Reference 8.
[b]Reference 39.
[c]References 13 and 14.

TABLE V. Observed transitions in the (100) excited vibrational state of CH_2.

Laser line (cm^{-1})[a]	Resonant field (T)	Assignment[b] $N_{K_aK_c}$	J	M_J	Obs.–Calc. (MHz)	(G)[c]	TR[d]	Int.[e]
61.3371	0.08510	2 1 1 ← 2 0 2	1 ← 1	−1 ← −1	32.2	+12.0	−2.68	572
61.3371	0.12610	2 1 1 ← 2 0 2	1 ← 1	0 ← 0	6.0	+5.2	−1.16	476
61.3371	0.22880	2 1 1 ← 2 0 2	1 ← 1	1 ← 1	6.4	+15.5	−0.42	6670
61.3371	0.04720	2 1 1 ← 2 0 2	1 ← 1	0 ← −1	−9.1	−4.7	−1.93	4261
61.3371	0.05200	2 1 1 ← 2 0 2	1 ← 1	1 ← 0	−10.6	−6.7	−1.57	4080
61.3371	0.07230	2 1 1 ← 2 0 2	3 ← 1	−2 ← −1	−19.8	−6.0	−3.29	181
61.3371	0.13840	2 1 1 ← 2 0 2	3 ← 3	−1 ← −2	−9.8	+3.7	2.62	443
61.3371	0.16870	2 1 1 ← 2 0 2	1 ← 1	−1 ← 0	−18.3	−13.5	−1.35	3024
61.3371	0.19000	2 1 1 ← 2 0 2	2 ← 3	2 ← 3	4.3	+9.1	−0.47	3309
61.3371	0.19220	2 1 1 ← 2 0 2	3 ← 3	3 ← 2	8.3	−5.0	1.66	1640
61.3371	0.75500	2 1 1 ← 2 0 2	1 ← 1	0 ← 1	−9.5	−71.3	−0.13	3929
63.0861	0.25600	3 1 2 ← 3 0 3	3 ← 3	−2 ← −2	7.4	−12.7	0.58	5756
63.0861	0.28183	3 1 2 ← 3 0 3	3 ← 3	−1 ← −1	4.7	−13.0	0.36	2718
63.0861	0.32872	3 1 2 ← 3 0 3	3 ← 3	0 ← 0	2.8	−11.7	0.24	652
63.0861	0.37758	3 1 2 ← 3 0 3	3 ← 3	3 ← 3	−7.6	+21.2	0.36	4017
63.0861	0.39804	3 1 2 ← 3 0 3	3 ← 3	2 ← 2	−4.1	+19.8	0.21	1051
63.0861	0.12437	3 1 2 ← 3 0 3	3 ← 3	−2 ← −3	−0.4	+0.3	1.47	1290
63.0861	0.14280	3 1 2 ← 3 0 3	3 ← 3	−1 ← −2	0.1	−0.1	1.03	2818
63.0861	0.17745	3 1 2 ← 3 0 3	3 ← 3	0 ← −1	−0.9	+1.3	0.66	4069
63.0861	0.18434	3 1 2 ← 3 0 3	2 ← 4	−1 ← 0	7.0	+3.8	−1.84	1531
63.0861	0.18661	3 1 2 ← 3 0 3	2 ← 4	−2 ← −1	−13.8	−5.7	−2.44	812
63.0861	0.23219	3 1 2 ← 3 0 3	3 ← 3	2 ← 3	−3.7	+5.1	0.71	3144
63.0861	0.25046	3 1 2 ← 3 0 3	4 ← 4	2 ← 3	−3.2	−3.4	−0.95	2532
63.0861	0.25967	3 1 2 ← 3 0 3	3 ← 3	1 ← 0	−1.0	+3.2	0.32	4844
63.0861	0.30848	3 1 2 ← 3 0 3	3 ← 3	1 ← 2	−1.8	+5.1	0.35	4672
63.0861	0.46075	3 1 2 ← 3 0 3	4 ← 4	1 ← 2	3.7	+21.1	−0.17	4096
63.0861	0.51610	3 1 2 ← 3 0 3	3 ← 3	0 ← 1	3.2	−28.8	0.11	5014
63.0861	0.66875	3 1 2 ← 3 0 3	4 ← 4	−1 ← −2	11.6	+92.3	−0.13	4071
63.0861	0.71271	3 1 2 ← 3 0 3	3 ← 3	2 ← 1	−4.0	+80.8	0.05	5048

[a]See Table I. 61.3371 cm^{-1} data from Mucha *et al.* (Ref. 23).
[b]The assignment given for J is that with which the given M_J level correlates at zero field.
[c]1 G (Gauss) = 10^{-4} T (Tesla).
[d]Calculated tuning rate of the given transition in MHz/G.
[e]Calculated relative line intensity, including rotational (but not vibrational) Botlzmann factor for 300 K.

perimental value for the (000) vibrational state includes the effects of zero-point motion. However, the effects of this vibrational averaging have been calculated to be quite small (0.0003 cm^{-1} for D and −0.0006 cm^{-1} for E).[13]

The spin-rotation interaction makes a small contribution to the fine structure splittings in CH_2, although the relative effect of this interaction increases with N. The absolute magnitudes of ϵ_{bb} and ϵ_{cc} can be estimated from the spin-orbit integrals calculated by Langhoff[14(b)] on the basis that second order contributions dominate. The resulting values of $|\epsilon_{bb}|(\text{calc}) = 0.0035$ cm^{-1} and $|\epsilon_{cc}|(\text{calc}) = 0.0026$ cm^{-1} are in reasonably good agreement with the experimental values in Table III.

C. Excited state rotational transitions

Two transitions have been assigned in the present study which do not belong to the ground vibrational state (000) of CH_2. One of these, which shows triplet hyperfine structure, is the spectrum observed at 61.337 cm^{-1} by Mucha *et al.*[23] and the other transition, which does not show hyperfine splitting, was observed using a nearby laser line at 63.086 cm^{-1} (see Table I). These spectra may be assigned to the rotational transitions $2_{11} - 2_{02}$ and $3_{12} - 3_{03}$, respectively, but they are located about 3.95 cm^{-1} below the corresponding ground state ones. Since they are not due to other isotopes of CH_2 (see Ref. 23), we interpret them as rotational transitions within an excited vibrational state. This excited state cannot be (010) or a higher bending level, for which these transitions occur at much higher frequency,[26] nor can it be the (001) asymmetric stretch level, for which hyperfine splitting would appear in $3_{12} - 3_{03}$ and not $2_{11} - 2_{02}$. The most likely assignment is to the (100) first excited symmetric stretching level. The observed resonances are listed in Table V with their detailed assignments, and the resulting adjusted molecular parameters for the (100) level are given in Table VI. Note that there are small but significant changes in the spin–spin and spin-rotation parameters between (000) and (100); the change in D is considerably larger than, and opposite in sign to, that predicted by Langhoff and Kern.[13] This difference may be a reflection of the problems associated with the treatment of the spin-orbit contributions to this quantity noted above. There is also a fairly large change in the A rotational constant; this is quite consistent with the assignment to the (100) state.

By comparing the intensities of LMR transitions within (000) and (100) observed on the same laser line

TABLE VI. Parameters for the (100) excited vibrational state of CH_2 ($\tilde{X}\,^3B_1$).

Parameter[a]	Value/cm^{-1}
A	69.116 65(49)
B	8.399 74(18)
D	0.785 88(111)
E	0.043 81(31)
ϵ_{bb}	−0.004 23(14)
ϵ_{cc}	−0.002 78(12)

[a]All other parameters were fixed at their ground (000) state values (see Table III).

(63.086 cm^{-1}) a very approximate population ratio of 10 : 1 for (000) : (100) is estimated. Since the (100) state is likely[42] to lie in the region of 3000 cm^{-1}, the effective vibrational temperature for this mode is well over 1000 K. Such a large departure from equilibrium suggests that CH_2 is directly formed in excited vibrational states in our apparatus and detected before it has a chance to relax significantly. Radiative decay from (100) to (000) is expected to be slow, since this transition is forbidden in the linear limit. Indeed, the *ab initio* dipole moment function calculated by Harding and Goddard[43] suggests a very small transition dipole moment of about 0.01 D for the (100)–(000) transition.

The observation of the (100) state reported here could be of special interest because some of the rotational levels of this state may be subject to perturbations from levels of the $\tilde{a}\,^1A_1$ state. The interpretation of such perturbations could lead to a direct and precise measurement of the singlet-triplet splitting in CH_2. It is even possible that the inverted spectra, apparently due to CH_2, which have been observed in the FIR LMR spectrum but not yet assigned,[44] may be perturbed rotational transitions either in excited vibrational levels of the $\tilde{X}\,^3B_1$ state or in the $\tilde{a}\,^1A_1$ state.

D. Determination of hyperfine parameters

Many of the observed transitions involving *ortho*-CH_2 show well-resolved triplet hyperfine structure and thus carry information about the proton nuclear hyperfine interaction. Examples of such triplets in the $4_{13} - 4_{04}$ transition are apparent in Fig. 3. We have taken a representative set of hyperfine splittings from the ground state transitions and fitted them by a least-squares procedure to determine the parameters in the effective Hamiltonian H_{hfs} given in Eq. (6). The calculations were performed in Southampton using the program described by Barnes *et al.*[34] We were not able to include all the observed LMR splittings in the data set because of the large amount of computation time involved, but we did incorporate the zero-field splittings measured by Lovas *et al.*[27] for the $4_{04} - 3_{13}$ microwave transition. The experimental LMR splittings used and the results of the fit are given in Table VII. The hyperfine parameters determined in the process are listed in Table III. The splittings are generally reproduced to within experimental error and all three main hyperfine parameters are determined.

In each case, the LMR hyperfine structure consists of an equally-spaced triplet of lines of equal intensity, even when the resonance occurs at low magnetic fields (0.01 T). This means that the nuclear spin is decoupled and there is an ambiguity in the assignment of the M_I quantum number for the LMR data, with a resulting ambiguity in the sign of the Fermi contact parameter a_{FC}. Fortunately, the observed intensities and splittings in the $4_{04} - 3_{13}$ microwave spectrum[27] leave no doubt as to the sign of a_{FC}, which is negative in accord with general expectations. In a simple picture, the triplet splitting arises from the interaction between the coupled proton magnetic moments and the unpaired electrons in $2p_x$ and $2p_y$ orbitals on the C atom. Assuming the molecule to be essentially linear, one would then expect the Fermi contact parameter to be zero since it depends on the unpaired electron spin density at the nuclei in question. A slightly more sophisticated calculation predicts the parameter to be small and negative, the interaction arising through spin polarization of the σ C–H bonds. Our result is consistent with this expectation.

A careful study of the residuals in Table VII shows that the fit is not completely satisfactory in that its quality does not quite match the experimental precision. There would appear to be some inconsistency between the LMR and zero-field data sets since fits of much better quality can be obtained by treating the data sets separately. It is worrying that the values for the hyperfine parameters, particularly the dipolar parameters, in Table III are significantly different from the set determined in an earlier fit of the LMR data alone. Unfortunately we have not been able to explain this discrepancy. We are convinced that it is not attributable to experimental error. We have also investigated the possibility that it might be caused by hyperfine mixing of the 4_{04} (*ortho*) and 3_{12} (*para*) levels through the T_{ab} term in the Hamiltonian in Eq. (6). It can be seen from Fig. 2 that these levels are quite close in energy (4.8 cm^{-1}). Numerical calculations reveal that a magnitude for the T_{ab} component of about 1 GHz is required to produce shifts of the 4_{04}–3_{13} frequencies of the right size. We consider this value to be unacceptably large. There is also a possibility that the discrepancy can be accommodated by the inclusion of centrifugal distortion corrections to the hyperfine Hamiltonian, particularly about the a inertial axis. However, we do not think this very likely since the fine structure splittings of the same levels do not show such effects.

In spite of these blemishes, it is worth considering the interpretation of the hyperfine parameters. The Fermi contact parameter a_{FC} is determined to be −20.3 MHz (see Table III), less than half of the corresponding parameter for CH in its $X\,^2\Pi$ state −57.4 GHz.[45] Such a large difference can be attributed to the slight nonlinearity of CH_2. The electron in the in-plane $2p$ methylene orbital has a small but nonzero density at each proton in CH_2 thus giving an offsetting positive contribution to a_{FC}. The dipolar hyperfine interaction is characterized by three principal components T_{aa}, T_{bb}, and T_{cc}. It can be seen from Table III that the tensor deviates only slightly from cylindrical symmetry (i.e., $T_{bb} \approx T_{cc}$

TABLE VII. Observed ^1H hyperfine splittings in $X\,^3B_1$ (000) CH_2.[a]

Assignment				Resonant	10^4 (Obs.−Calc.)
$N_{K_aK_c}$	J	M_J	M_F	field (T)	(T)
$1_{11} \leftarrow 2_{02}$	2 ← 3	−2 ← −1	−3 ← −2	0.013 66	−0.9
			−1 ← 0	0.014 98	0.8
$1_{11} \leftarrow 2_{02}$	1 ← 1	−1 ← 0	−2 ← 1	0.071 67	1.7
			0 ← 1	0.074 05	−1.9
$1_{11} \leftarrow 2_{02}$	2 ← 3	−1 ← 0	−2 ← −2	0.036 60	2.6
			0 ← 0	0.039 60	−1.9
$1_{11} \leftarrow 2_{02}$	2 ← 3	−1 ← 0	−2 ← −1	0.020 51	−0.7
			0 ← 1	0.022 22	0.3
$2_{11} \leftarrow 2_{02}$	2 ← 1	0 ← 0	−1 ← −1	0.588 61	0.0
			1 ← 1	0.589 79	0.0
$2_{11} \leftarrow 2_{02}$	2 ← 3	−2 ← −3	−3 ← −4	1.057 10	1.4
			−1 ← −2	1.059 14	−1.5
$2_{11} \leftarrow 2_{02}$	2 ← 1	−1 ← −1	−2 ← −2	1.010 26	−0.6
			0 ← 0	1.011 68	1.2
$2_{11} \leftarrow 2_{02}$	2 ← 1	2 ← 1	1 ← 0	0.910 48	−0.8
			3 ← 2	0.912 42	0.1
$4_{13} \leftarrow 4_{04}$	5 ← 4	−4 ← −4	−5 ← −5	0.028 11	2.2
			−3 ← −3	0.030 78	−2.1
$4_{13} \leftarrow 4_{04}$	3 ← 5	2 ← 2	1 ← 1	0.421 71	2.0
			3 ← 3	0.423 87	−1.0
$4_{13} \leftarrow 4_{04}$	3 ← 4	−3 ← −4	−4 ← −5	0.008 99	−0.4
			−2 ← −3	0.010 84	−1.3
$4_{13} \leftarrow 4_{04}$	5 ← 5	4 ← 5	3 ← 4	0.644 86	0.0
			5 ← 6	0.647 01	−0.3
$1_{11} \leftarrow 0_{00}$	1 ← 1	1 ← 1	0 ← 0	0.157 01	−1.0
			2 ← 2	0.158 29	1.3
$1_{11} \leftarrow 0_{00}$	1 ← 1	0 ← 0	−1 ← −1	0.204 06	0.0
			1 ← 1	0.205 50	0.8
$1_{11} \leftarrow 0_{00}$	1 ← 1	−1 ← 1	−2 ← −1	0.156 61	0.9
			0 ← 2	0.158 74	−1.3
$1_{11} \leftarrow 0_{00}$	2 ← 1	0 ← 1	−1 ← 0	0.307 21	−2.1
			1 ← 2	0.308 68	1.0
$6_{15} \leftarrow 6_{06}$	6 ← 5	1 ← 1	0 ← 0	0.372 86	−1.1
			2 ← 2	0.374 06	1.7
$6_{15} \leftarrow 6_{06}$	6 ← 5	−3 ← −3	−4 ← −4	0.376 54	−1.5
			−2 ← −2	0.378 09	1.0
$6_{15} \leftarrow 6_{06}$	6 ← 5	−2 ← −2	−3 ← −3	0.379 71	−0.3
			−1 ← −1	0.380 99	2.2
$6_{15} \leftarrow 6_{06}$	6 ← 5	−1 ← −1	−2 ← −2	0.382 06	−1.4
			0 ← 0	0.386 19	1.5
$3_{22} \leftarrow 4_{13}$	2 ← 3	2 ← 2	1 ← 1	0.109 55	1.2
			3 ← 3	0.111 26	−0.8
$3_{22} \leftarrow 4_{13}$	2 ← 3	1 ← 1	0 ← 0	0.121 16	0.9
			2 ← 2	0.122 67	−0.2
$3_{22} \leftarrow 4_{13}$	4 ← 3	3 ← 3	2 ← 2	0.206 41	1.3
			4 ← 4	0.208 83	−2.0
$3_{22} \leftarrow 4_{13}$	3 ← 3	2 ← 2	1 ← 1	0.243 83	0.3
			3 ← 3	0.245 91	−0.6
$4_{22} \leftarrow 5_{15}$	4 ← 4	4 ← 4	3 ← 3	0.180 13	0.7
			5 ← 5	0.182 08	−0.8
$4_{22} \leftarrow 5_{15}$	4 ← 6	4 ← 4	3 ← 3	0.566 35	0.5
			5 ← 5	0.567 15	0.0
$4_{22} \leftarrow 5_{22}$	4 ← 6	5 ← 5	4 ← 4	0.725 77	1.6
			6 ← 6	0.727 04	−0.5

[a]Only the LMR data included in the fit to the hyperfine parameters are given here. Field positions for the central component of the hyperfine triplets are given in Table II. Also incorporated in the fit were the hyperfine splittings measured at zero field for the 4_{04}–3_{13} transition (Ref. 27, see the text).

$= -[T_{aa} + T_{bb}]$), a manifestation of the near linearity of CH_2. Both the magnitude and sign of the components of **T** are consistent with the corresponding quantities for CH, $T_{\parallel} = 38.2$ MHz and $T_{\perp} = -19.1$ MHz.[45]

V. DISCUSSION AND CONCLUSIONS

We have reported here the observation of components of 13 pure rotational transitions in the ground vibronic

TABLE VIII. Calculated energy levels (without hyperfine splittings) for the ground vibronic state of CH_2 (in cm^{-1}).[a]

$N_{K_aK_c}$	F_1	F_2	F_3
0_{00}	−0.0029[b]		
1_{01}	15.5749	15.8973	15.1236
1_{11}	78.3385	78.2078	78.5439
1_{10}	79.5411	79.3638	79.8198
2_{02}	46.7891	47.1384	46.6308
2_{12}	108.4072	108.6116	108.3241
2_{11}	111.9980	112.1528	111.9463
2_{21}	276.3551	276.0242	276.5484
2_{20}	276.3738	276.0424	276.5674
3_{03}	93.5694	93.9361	93.4831
3_{13}	153.5551	153.8583	153.4860
3_{12}	160.7135	160.9656	160.6667
3_{22}	323.4371	323.4500	323.4618
3_{21}	323.5300	323.5417	323.5552
4_{04}	155.8359	156.2159	155.7880
4_{14}	213.7291	214.0790	213.6840
4_{13}	225.6206	225.9188	225.5944
4_{23}	386.2170	386.3779	386.2160
4_{22}	386.4933	386.6520	386.4931
5_{05}	233.4905	233.8816	233.4689
5_{15}	288.8835	289.2612	288.8598
5_{14}	306.6551	306.9808	306.6484
5_{24}	464.6233	464.8641	464.6249
5_{23}	465.2613	465.4987	465.2640
6_{06}	326.4177	326.8187	326.4164
6_{16}	378.9691	379.3659	378.9638
6_{15}	403.7440	404.0888	403.7549
6_{25}	558.5866	558.8768	558.5980
6_{24}	559.8466	560.1321	559.8596

[a]The energies are not necessarily reliable to the quoted precision of 0.0001 cm^{-1}. However, transition frequencies corresponding to those observed (Table II) should approach this accuracy.

[b]The 0_{00} energy level is shifted slightly from zero by spin–spin interaction with the F_3 component of 2_{02}.

state of the methylene radical, and an additional two transitions in an excited vibrational state believed to be (100). Inspection of Fig. 2 shows that a large fraction of the possible transitions involving rotational levels with energies less than 500 cm^{-1} have been observed. In Table VIII, we present a list of energy levels calculated using the constants of Table III and neglecting the small hyperfine splittings.

It would be desirable to extend the study of the LMR spectrum of CH_2 to observe transitions involving levels with $K_a \geq 3$. Such transitions lie at higher frequencies ($\gtrsim 200$ cm^{-1}) where there are relatively few laser lines currently available for use in the LMR apparatus. The number of such laser lines is likely to increase in the next few years.

The data reported here together with the ν_2 band LMR spectrum[24,26] enable the geometrical structure of CH_2 to be estimated by means of the semirigid bender model. This calculation is described in detail by Sears *et al.*[26] and the resulting structure, averaged over the ground state bending and stretching motions, is $R_0 = 1.085$ Å and $\alpha_0 = 135.5°$.

Further experiments involving the related isotopic species CD_2 and CHD are planned. Information on the rotational spectra of these molecules will enable more detailed determinations of the geometrical and electronic structure of methylene. We also hope to extend the measurements of rotational transitions in excited vibrational states of CH_2. As mentioned above, such observations may ultimately lead to an unambiguous determination of the singlet–triplet splitting in methylene.

ACKNOWLEDGMENTS

We wish to acknowledge the efforts of J. A. Mucha and R. J. Saykally during extensive preliminary searches for LMR spectra of CH_2 which optimized the chemistry for producing methylene and produced spectra in vibrationally excited states. We also acknowledge J. T. Hougen for many stimulating discussions and calculations made in attempting to assign the early CH_2 results. We are grateful to S. C. Ross and M. J. Bush for help with the calculations and to L. B. Harding for communicating details of *ab initio* calculations on CH_2.

[1]G. Herzberg and J. Shoosmith, Nature (London) **183**, 1801 (1959).
[2]G. Herzberg, Proc. R. Soc. London Ser. A **262**, 291 (1961).
[3]G. Herzberg and J. W. C. Johns, Proc. R. Soc. London Ser. A **295**, 707 (1966).
[4]R. A. Bernheim, H. W. Bernard, P. S. Wang, L. S. Wood, and P. S. Skell, J. Chem. Phys. **53**, 1280 (1970); **54**, 3223 (1970).
[5]E. Wasserman, W. A. Yager, and V. J. Kuck, Chem. Phys. Lett. **7**, 409 (1970).
[6]E. Wasserman, V. J. Kuck, R. S. Hutton, and W. A. Yager, J. Am. Chem. Soc. **92**, 7491 (1970).
[7]E. Wasserman, V. J. Kuck, R. S. Hutton, E. D. Anderson, and W. A. Yager, J. Chem. Phys. **54**, 4120 (1971).
[8]E. Wasserman, R. S. Hutton, V. J. Kuck, and W. A. Yager, J. Chem. Phys. **55**, 2593 (1971).
[9]G. Herzberg and J. W. C. Johns, J. Chem. Phys. **54**, 2276 (1971).
[10](a) C. F. Bender and H. F. Schaefer III, J. Am. Chem. Soc. **92**, 4984 (1970); (b) D. R. McLaughlin, C. F. Bender, and H. F. Schaefer III, Theor. Chim. Acta **25**, 352 (1972).
[11]J. F. Harrison and L. C. Allen, J. Am. Chem. Soc. **91**, 807 (1969).
[12]J. F. Harrison, Acc. Chem. Res. **7**, 378 (1974).
[13]S. R. Langhoff and C. W. Kern, in *Modern Theoretical Chemistry*, edited by H. F. Schaefer (Plenum, New York, 1977), Vol. IV.
[14](a) S. R. Langhoff and E. R. Davidson, Int. J. Quantum Chem. **7**, 579 (1973); (b) S. R. Langhoff, J. Chem. Phys. **61**, 3881 (1974).
[15](a) L. B. Harding and W. A. Goddard III, Chem. Phys. Lett. **55**, 217 (1978); (b) S.-K. Shih, D. Peyerimhoff, R. J. Buenker, and M. Peric, Chem. Phys. Lett. **55**, 206 (1978).
[16]P. Saxe, H. F. Schaefer III, and N. C. Handy, J. Phys. Chem. **85**, 745 (1981).
[17]J. W. Simons and R. Curry, Chem. Phys. Lett. **38**, 171 (1976).
[18]R. K. Lengel and R. N. Zare, J. Am. Chem. Soc. **100**, 7495 (1978).
[19]C. C. Hayden, D. M. Neumark, K. Shobatake, R. K. Sparks, and Y. T. Lee, J. Chem. Phys. **76**, 3607 (1982).
[20]P. F. Zittel, G. B. Ellison, S. V. O'Neil, E. Herbst, W. C. Lineberger, and W. P. Reinhardt, J. Am. Chem. Soc. **98**, 3731 (1976).

[21]P. C. Engelking, R. R. Corderman, J. J. Wendoloski, G. B. Ellison, S. V. O'Neil, and W. C. Lineberger, J. Chem. Phys. **74**, 5460 (1981).
[22](a) J. Danon, S. V. Filseth, D. Feldmann, H. Zacharias, C. H. Dugan, and K. H. Welge, Chem. Phys. **29**, 345 (1978); (b) D. Feldmann, K. Meier, H. Zacharias, and K. H. Welge, Chem. Phys. Lett. **59**, 171 (1978).
[23]J. A. Mucha, K. M. Evenson, D. A. Jennings, G. B. Ellison, and C. J. Howard, Chem. Phys. Lett. 66, 244 (1979).
[24]T. J. Sears, P. R. Bunker, and A. R. W. McKellar, J. Chem. Phys. **75**, 4731 (1981).
[25]P. R. Bunker and B. M. Landsberg, J. Mol. Spectrosc. **67**, 374 (1977).
[26]T. J. Sears, P. R. Bunker, A. R. W. McKellar, J. Chem. Phys. **77**, 5363 (1982).
[27]F. J. Lovas, R. D. Suenram, and K. M. Evenson (to be published).
[28]K. M. Evenson, R. J. Saykally, D. A. Jennings, R. F. Curl, and J. M. Brown, in *Chemical and Biochemical Applications of Lasers*, edited by C. B. Moore (Academic, New York, 1980), Vol. 5, p. 95; K. M. Evenson, D. A. Jennings, F. R. Peterson, J. A. Mucha, J. J. Jimenez, R. M. Charlton, and C. J. Howard, IEEE J. Quantum Electron. **QE-13**, 442 (1977).
[29]J. H. Van Vleck, Rev. Mod. Phys. **23**, 213 (1951).
[30]W. T. Raynes, J. Chem. Phys. **41**, 3020 (1964).
[31]I. C. Bowater, J. M. Brown, and A. Carrington, Proc. R. Soc. London Ser. A **333**, 265 (1973).
[32]J. K. G. Watson, in *Vibrational Spectra and Structure*, edited by J. R. Durig (Elsevier, New York, 1977), Vol. 6, p. 1.
[33]J. M. Brown and T. J. Sears, J. Mol. Spectrosc. **75**, 111 (1979).
[34]C. E. Barnes, J. M. Brown, A. Carrington, J. Pinkstone, T. J. Sears, and P. J. Thistlethwaite, J. Mol. Spectrosc. **72**, 86 (1978).
[35]J. C. D. Brand, C. DiLauro, and D. S. Liu, Can. J. Phys. **53**, 1853 (1975).
[36]J. M. Brown, P. R. Bunker, K. M. Evenson, D. A. Jennings, F. J. Lovas, A. R. W. McKellar, and T. J. Sears (to be published).
[37]R. F. Curl, Mol. Phys. **9**, 585 (1965).
[38]For example: F. W. Birss, D. A. Ramsay, S. C. Ross, and C. Zauli, J. Mol. Spectrosc. **78**, 344 (1979).
[39]B. R. Bicknell, W. R. M. Graham, and W. Weltner, J. Chem. Phys. **64**, 3319 (1976).
[40]R. A. Bernheim, T. Adl, H. W. Bernard, A. Songco, P. S. Wang, R. Wang, L. S. Wood, and P. S. Skell, J. Chem. Phys. **64**, 2747 (1976).
[41]P. Phillips and E. R. Davidson, J. Chem. Phys. **76**, 516 (1982).
[42]Y. Osamura, Y. Yamaguchi, and H. F. Schaefer III, J. Chem. Phys. **75**, 2919 (1981).
[43]L. B. Harding (private communication, 1981).
[44]K. M. Evenson, R. J. Saykally, and J. T. Hougen, Paper TF-5. 34th Symposium on Molecular Spectroscopy, Columbus, Ohio, 1979.
[45]J. T. Hougen, J. A. Mucha, D. A. Jennings, and K. M. Evenson, J. Mol. Spectrosc. **72**, 463 (1978); J. M. Brown and K. M. Evenson (to be published).